

Active Learning of Spin Network Models

Jialong Jiang^a, David A. Sivak^b, and Matt Thomson^{a,1}

^aDivision of Biology and Biological Engineering, California Institute of Technology, Pasadena, CA 91125; ^bDepartment of Physics, Simon Fraser University, Burnaby, BC V5A 1S6, Canada

This manuscript was compiled on December 20, 2024

Complex networks can be modeled as a probabilistic graphical model, where the interactions between binary variables, "spins", on nodes are described by a coupling matrix that is inferred from observations. The inverse statistical problem of finding direct interactions is difficult, especially for large systems, because of the exponential growth in the possible number of states and the possible number of networks. In the context of the experimental sciences, well-controlled perturbations can be applied to a system, shedding light on the internal structure of the network. Therefore, we propose a method to improve the accuracy and efficiency of inference by iteratively applying perturbations to a network that are advantageous under a Bayesian framework. The spectrum of the empirical Fisher information can be used as a measure for the difficulty of the inference during the training process. We significantly improve the accuracy and efficiency of inference in medium-sized networks based on this strategy with a reasonable number of experimental queries. Our method could be powerful in the analysis of complex networks as well as in the rational design of experiments.

Network | Inference | Active Learning | Information Geometry

A significant property of complex systems is the convoluted interaction between different parts. Describing the structure of interactions in the network is critical to understanding and predicting its behavior. Numerous models have been developed to characterize complex networks, and many different methods are used to infer network interactions from the data generated by a network, such as correlation, mutual information, likelihood, or dynamics (1). Among all of these approaches, spin network models are one of the simplest and most natural in the sense of that such models provide the maximum entropy inference of a network given the means and correlations of nodes in network (2). The inference problem involved in parametrizing a spin network model from data is known as the inverse Ising problem (or spin glass inverse problem) in physics, and has been widely applied to many fields such as computational biology (3, 4), neuroscience (5), data science (6), etc. (2)

A spin network is a probabilistic graphical model with each node taking value in $\{1, -1\}$. For a p -node network, the probability of 2^p configurations is the induced Boltzmann distribution from an Ising-type interaction energy. For simplicity, the inverse temperature factor β is absorbed into the parameters for interactions and field strengths. Then the probability of a configuration \mathbf{s} given an interaction matrix \mathbf{J} and local field \mathbf{h} is

$$P(\mathbf{s}|\mathbf{J}, \mathbf{h}) = \frac{\exp[-E(\mathbf{s})]}{\mathcal{Z}},$$

$$E(\mathbf{s}) = -\sum_{i<j} J_{ij} s_i s_j - \sum_i h_i s_i, \quad [1]$$

where $\mathcal{Z} = \sum_{\{\mathbf{s}\}} \exp[-E(\mathbf{s})]$ is the partition function. The learning or inference of the model means finding the best \mathbf{J}

and \mathbf{h} to describe the observed data, which can be solved by maximum likelihood estimation (MLE), pseudo-likelihood (7) or other approximate optimization methods (8).

To solve the inverse Ising problem is hard both in sampling complexity and computational cost (9, 10). Even though MLE is a convex optimization problem, the Hessian matrix can be close to singular (11), making it difficult to distinguish alternatives of parameter values. A canonical demonstration is a 3-node network whose three nodes are all strongly correlated, as shown in Fig. 1 (a). All interactions have the same strength $J > 0$, so the correlation between any pair of nodes is close to 1 with large J . The difference in correlation caused by different network structures decreases exponentially with the coupling strength, as shown in Fig. 1 (b). Considering that the correlations and means are sufficient statistics of the problem, it is almost impossible to find the correct structure without extra information. Examples could be constructed to show that any algorithm has a high probability to fail under some conditions (10). Detailed analysis of sampling complexity shows that the number of samples needed to distinguish different structures grows polynomially with the number of edges, but exponentially with ℓ_∞ norm of \mathbf{J} , which represents the coupling strength between nodes (9).

Those difficulties are not specific to this model, but generally confronted while deducing causation from correlation. Many disciplines in scientific research rely on perturbations to tackle the causal inference problem, especially biology. For example, gene functions are studied by their mutants, and signaling pathways are decoded from carefully designed knock

Significance Statement

The inverse problem of learning causation from correlation is always difficult. In natural sciences, this issue is tackled by applying interventions to a system to reveal hidden information. Development of new technologies now enables the performance of high-throughput perturbation experiments to probe network structure in many fields. However, the analysis and design of such experiments still remains mostly empirical. We developed an inference framework that allows automated and active learning of network models through iterative rounds of observation and perturbation. New perturbations are rationally designed to improve our knowledge of the currently most uncertain part of a network. The learning process actively explores the behavior of a given system and combines all information to obtain a complete picture. Our formulation of the problem also raises new statistical problems for further investigation.

The authors declare no conflict of interest.

¹To whom correspondence should be addressed. E-mail: mthomson@caltech.edu

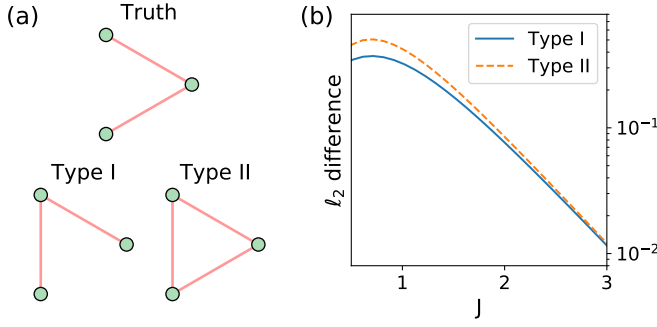


Fig. 1. The difficulty of inferring a three-node network. (a) During network inference, two common types of error could occur. Type I error occurs when some correct edges are missing and the inference may contain incorrect edges in compensation. This is because different interaction topologies may result in a similar correlation pattern in data. Type II error occurs when the inferred network includes extra incorrect interaction edges, which is related to correlations between nodes caused by indirect interactions. (b) The spin-spin correlations in data generated by the three different networks from (a) with high interaction strengths are nearly identical. The ℓ_2 difference of correlation vectors caused by the two types of incorrect structures is plotted as a function of J , where all interaction strengths are set to J . The ℓ_2 difference decreases exponentially with J , so distinguishing different structures is extremely difficult with sampling noise.

in/off experiments. Recent developments in molecular biology provide high-throughput technology to perform perturbation experiments, such as CRISPER/Cas9 in gene editing (12, 13) and optogenetics in neuron activity control (14). With these methods, it is natural to ask how to design perturbation experiments and extract information from the data to make the best possible inference. Similar ideas have been proposed in the context of Boolean networks with only population average data, which is more restricted in capturing the distribution properties and interaction intensities (15). Although there has been research on optimal design (16) and analysis (17) of experiments, a general framework for combining the two processes is still absent, especially for the inverse Ising problem discussed in this paper.

In this paper, we propose a framework to learn the coupling matrix \mathbf{J} in the inverse Ising problem by iteratively updating our knowledge through designed perturbation experiments. We demonstrate procedures for designing experiments and a learning process to achieve significant improvement in inference accuracy on medium-sized networks under strong couplings. This method provides new insights into the spin network model, and can be applied to complex networks in real systems.

Formulation of Inference with Perturbations

The most common perturbations applicable in real situations are individually activating/deactivating different nodes, such as knockdown of genes, induced activation of neurons, etc. In a spin network, the local field \mathbf{h} describes a tendency of activation for every node. Specifically,

$$\frac{P(s_i = 1)}{P(s_i = -1)} \bigg|_{h_i = h} = \frac{P(s_i = 1)}{P(s_i = -1)} \bigg|_{h_i = 0} \exp(2h). \quad [2]$$

Therefore, the perturbation can be modeled by the effect of the local field \mathbf{h} , which we are able to control to facilitate the inference of \mathbf{J} . For simplicity, we assume that we have full control of the field, namely the system does not have an unknown intrinsic field. The case with an intrinsic field can be dealt with similarly using the framework we developed.

Quantification of the difficulty of inference is necessary to design a field that alleviates it, and information geometry provides such a measure. Information geometry defines a geometric structure to characterize the change in a probability distribution with changes in underlying parameters. For a parametric family of distribution $P(\mathbf{x}|\boldsymbol{\theta})$, the difference between any two distributions measured by Kullback-Leibler divergence can be expanded as a series of $\delta\boldsymbol{\theta}$

$$\text{KL}(P(\mathbf{x}|\boldsymbol{\theta}), P(\mathbf{x}|\boldsymbol{\theta} + \delta\boldsymbol{\theta})) = \frac{1}{2} \delta\boldsymbol{\theta}^T \mathcal{I} \delta\boldsymbol{\theta} + \mathcal{O}(\delta\boldsymbol{\theta}^3)$$

$$\mathcal{I} = \left\langle \frac{\partial^2 \log P(\mathbf{x}|\boldsymbol{\theta})}{\partial \theta_i \partial \theta_j} \right\rangle = \left\langle \frac{\partial \log P}{\partial \theta_i} \frac{\partial \log P}{\partial \theta_j} \right\rangle. \quad [3]$$

The Fisher information matrix (FI) \mathcal{I} describes how the parametric density manifold curves. For independent samples, FI is additive. When the change in a distribution given changes in parameter values is small, the FI is "small", and inference is difficult. This phenomenon is characterized by Cramér–Rao bound which states that the covariance C of any unbiased estimator is no smaller than \mathcal{I}^{-1} in the sense of $C - \mathcal{I}^{-1}$ being positive semidefinite. One corollary is that $\Omega(\epsilon^{-1} \lambda^{-1})$ samples are needed to achieve error ϵ in expectation on the projection to an eigenvector of FI with eigenvalue λ . On the other hand, FI is also the expectation of the Hessian matrix of the log-likelihood function, representing the difficulty of numerical optimization of the likelihood function.

As the covariance of an estimator is related to the ℓ_2 error of estimation, the following problem statement

$$\begin{aligned} \min_{\mathbf{h}} \quad & \mathbb{E}(\|\mathbf{J} - \tilde{\mathbf{J}}\|_2) \\ \text{s.t.} \quad & \mathbf{s} \sim P(\mathbf{s}|\mathbf{J}, \mathbf{h}) \\ & \tilde{\mathbf{J}} = \underset{\mathbf{J}'}{\text{argmax}} \log P(\{\mathbf{s}\}|\mathbf{J}', \mathbf{h}) \end{aligned} \quad [4]$$

can be tackled by minimizing an asymptotic lower bound, the trace of inverse of FI using the applied field

$$\min_{\mathbf{h}} \quad \text{Tr} \mathcal{I}(P(\mathbf{s}|\mathbf{J}, \mathbf{h}))^{-1}. \quad [5]$$

For inverse Ising inference, the FI can be derived from properties of the exponential family of distributions

$$I_{\{ij\}, \{kl\}} = \langle s_i s_j s_k s_l \rangle - \langle s_i s_j \rangle \langle s_k s_l \rangle, \quad [6]$$

where $\{ij\}$ corresponds to interaction term J_{ij} . For the diagonal terms, $I_{\{ij\}, \{ij\}} = 1 - \langle s_i s_j \rangle^2$, the maximum is achieved when the correlation between two spin s_i, s_j is close to 0. There is a lower bound of $\text{Tr} \mathcal{I}^{-1}$ given by

$$\text{Tr} \mathcal{I}^{-1} \geq \frac{p^2}{\text{Tr} \mathcal{I}} \geq p, \quad [7]$$

which would be achieved when all configurations have the same probability. The optimal value of $\text{Tr} \mathcal{I}^{-1}$ can also be achieved by other distributions, and whether such distributions can be satisfied by an \mathbf{h} depends on the structure of the network. In some cases, suitable external fields can be analytically or numerically solved.

For the simplest case, FI of two-spin inference is a scalar, so the optimal is achieved at the maximum of \mathcal{I} , where $\langle s_1 s_2 \rangle = 0$. Without the field, $\mathcal{I} = 1 - \tanh^2 J = 1/\cosh^2 J$, which decays with J exponentially. The solution of $\langle s_i s_j \rangle = 0$ is

$$h_2 = \frac{1}{2} \log \frac{1 - \exp(2J + 2h_1)}{\exp 2J - \exp 2h_1}. \quad [8]$$

The optimal $\mathcal{I} = 1$ can be achieved by an infinite number of (h_1, h_2) , and one special solution is $h_1 = -h_2 = J + \log \sqrt{2}$ under the approximation of large positive J . By adding the field, FI is increased by a factor exponential in J , which means the sampling complexity is reduced exponentially.

The landscape of \mathcal{I} as a function of h_1, h_2 is shown in Fig. 2 (a) when $J = 1$. A remark is that this landscape is nonconvex and the maximum is not unique. The point without field ($h_1 = 0, h_2 = 0$) is a saddle point, with two principle axis directions $(1, 1)$ and $(1, -1)$, and \mathcal{I} along these two directions are shown in Fig. 2 (b). Intuitively, the difficulty of inference is caused by the high probability of ground state configurations and the corresponding diminishing probability of higher energy excited states. Fields in the direction of $(1, -1)$ will make one of the previous high energy states more accessible, thus increasing FI. On the other hand, the direction of $(1, 1)$ will make the distribution more concentrated to one state, and the FI would decrease, thus forming a saddle point.

Another canonical model is the finite ferromagnetic Ising chain with periodical boundary condition. For an analytical solution, we restrict ourselves to the case of knowing the chain structure and inferring the magnitude of individual interaction strengths. The energy function is

$$E = - \sum_{i=1}^p J_i s_i s_{i+1} - \sum_{i=1}^p h_i s_i, \quad [9]$$

where the convention of $s_{p+1} \equiv s_1$ is used. The FI can be solved approximately when $J_i > 0$ are all equal, and $h_i = 0$

$$\mathcal{I}_{\{i, i+1\}\{j, j+1\}} = \begin{cases} 4(p-1) \exp(-4J) & i = j \\ 4 \exp(-4J) & i \neq j \end{cases} \quad [10]$$

The FI is a circular matrix so its eigenvectors are the Fourier coefficients and there is one larger eigenvalue $\lambda_1 = 8(p-1) \exp(-4J)$ and $p-1$ degenerate small eigenvalues $\lambda_2 = 4(p-2) \exp(-4J)$, as shown in Fig. 2 (c). By the symmetry of the system and motivation from the two-node case, a possible good perturbation $h^{(1)}$ can be chosen as $h_i^{(1)} = h_0^{(1)}(-1)^i$, and $h_0^{(1)}$ is obtained by numerical optimization. The resulting eigenvalues are shown in Fig. 2 (c). Most eigenvectors have increased eigenvalues except one, which provides significant improvement for inference, but the remaining one eigenvalue may still cause difficulty. This example shows that a single perturbation sometimes is not sufficient to obtain large eigenvalues for all eigenvectors. However, as FI is additive for independent samples, we can combine the information from many samples with different choices of local fields. In the geometric viewpoint, eigenvectors with small eigenvalues in the FI represent flat, singular valleys with diminishing second-order derivative and, therefore, low local curvature in the likelihood landscape. Combining samples taken from different conditions is equivalent to adding these landscapes together. As the singular dimensions will differ for different applied perturbations, combining the landscape can make the overall landscape well-behaved. In the Ising chain example, another field $h^{(2)}$ with $h_i^{(2)} = h_0^{(2)} \cos(\pi i/2)$ can be used to improve the eigenvalue on the previous degenerate direction. Neither can $h^{(1)}$ nor $h^{(2)}$ improve eigenvalues in all eigenvectors, but the sum of the two FI improves all eigenvalues, as shown in Fig. 2 (c).

Iterative Bayesian Inference

To perform inference across a combination of different perturbations in a general setting, information obtained from different perturbations must be integrated. The inside argmax optimization problem in Eq. 4 is difficult, as the partition function \mathcal{Z} in the objective function involves exponentially many terms. For optimization, the gradient of the log-likelihood has a closed-form expression

$$\frac{\partial \log \mathcal{L}}{\partial J_{ij}} = \langle s_i s_j \rangle^o - \langle s_i s_j \rangle, \quad [11]$$

where the $\langle s_i s_j \rangle^o$ is the average over the observed samples, and $\langle s_i s_j \rangle$ is the average over the distribution generated by the current parameters. Even though exact evaluation still involves exponentially many terms, the gradient can be approximated by samples taken from Monte Carlo Markov chain sampling. In general, the inference cannot converge to the ground truth because of the accumulation of sampling error and the singularity of FI, and that is where perturbations can help.

Maximum likelihood estimation can be viewed as maximizing the probability over the Bayesian posterior. The inference process not only finds the most probable parameters, but also updates the posterior probability of each parameter J given the samples observed. The difficulty is that Bayesian inference can be computationally intractable if we need to compute and save the whole posterior each time. However, the gradient of log posterior can be computed by the recursive formula Eq. 14. In the equation, \mathcal{L}_n is just the same likelihood function as in single round learning, while P_{n-1} is the posterior of the previous round. The normalizing factor Z_n does not contribute to the gradient. The computational cost of the Bayesian gradient only linearly depends on the number of learning rounds. The log likelihood is additive, and the final landscape defined by the posterior is the superposition of the landscapes for each individual round of query.

Intuitively, our knowledge of the system will increase in this process, which can be proved by properties of FI. According to Cramér-Rao bound, the ℓ_2 error of inference is determined by $\text{Tr} \mathcal{I}^{-1}$. By properties of positive semidefinite matrices, $A \succeq B \Leftrightarrow A^{-1} \preceq B^{-1}$. Therefore

$$\text{Tr}(\mathcal{I}_1 + \mathcal{I}_2)^{-1} - \text{Tr} \mathcal{I}_1^{-1} = \text{Tr}((\mathcal{I}_1 + \mathcal{I}_2)^{-1} - \mathcal{I}_1^{-1}) \leq 0. \quad [15]$$

Thus, the lower bound of the ℓ_2 error of the estimator decreases with more training rounds.

The choice of perturbation \mathbf{h} is critical to improving the inference accuracy. As mentioned, $\text{Tr} \mathcal{I}^{-1}$ serves as a lower bound for the ℓ_2 error of any unbiased estimator. With $\mathbf{h}_i, i = 1, \dots, n-1$ already set, choice of \mathbf{h}_n in n -th round should be the solution of the optimization problem

$$\begin{aligned} \min_{\mathbf{h}_n} \quad & \text{Tr} \mathcal{I}_n^{-1} \\ \text{s.t.} \quad & \mathcal{I}_i = \mathcal{I}_{i-1} + \mathcal{I}(\mathbf{J}, \mathbf{h}_i) \quad i = 1, \dots, n \\ & \mathcal{I}_0 = 0, \end{aligned} \quad [16]$$

where \mathcal{I}_n is defined recursively. However, in real cases, $\mathcal{I}(\mathbf{J}, \mathbf{h}_i)$ cannot be evaluated directly as \mathbf{J} is unavailable. So we need to approximate $\mathcal{I}(\mathbf{J}, \mathbf{h}_n)$ with our current estimation $\hat{\mathbf{J}}$. For $i = 1, \dots, n-1$, we already acquired samples from the real system, thus \mathcal{I}_i can be approximated using the empirical

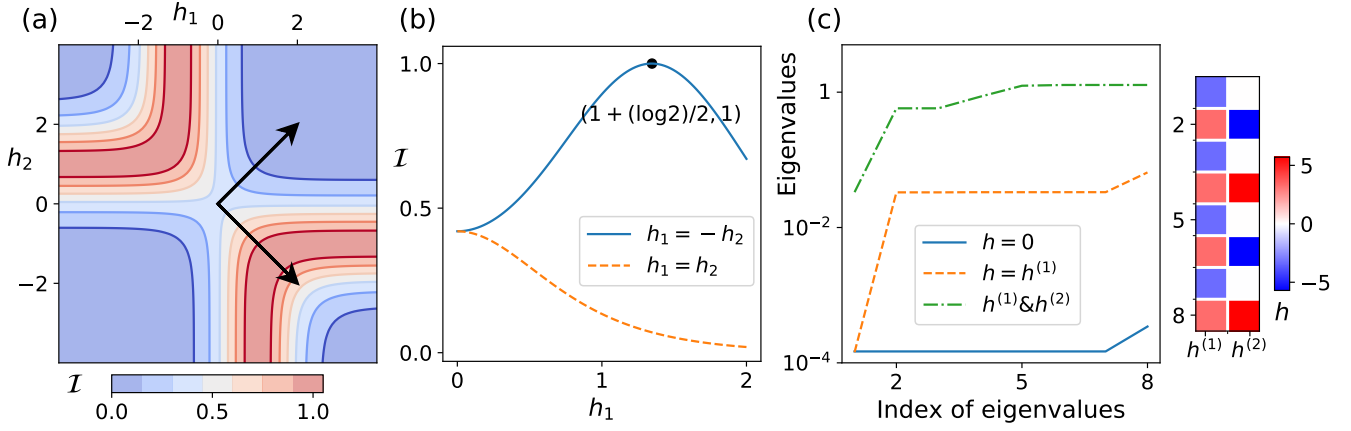


Fig. 2. Examples of two-node inference and Ising chain inference. The interaction $J = 1$ in (a)(b). (a) Landscape of the Fisher information \mathcal{I} with different applied field perturbations h_1, h_2 . Two arrows show the two main directions (eigenvectors of the Hessian matrix) of the saddle point at the origin, along which the FI is plotted in (b). (b) Fisher information as a function of h_1 when setting $h_1 = -h_2 \geq 0$ or $h_1 = h_2 \geq 0$. In the first case the maximum $\mathcal{I} = 1$ is achieved at $h_1 = J + \log \sqrt{2}$. (c) Eigenvalues of 1-dimensional ferromagnetic Ising model with $p = 8, J = 3$. When no field is applied, all eigenvalues are very small. When the field $h^{(1)}$ applied, all eigenvalues increase significantly except one. Combined with another field $h^{(2)}$, all eigenvalues are within a suitable range for precise inference.

$$P_n \equiv P(\mathbf{J} | \bigcup_{i=1}^n \{\mathbf{s}_i, \mathbf{h}_i\}) = \frac{P(\{\mathbf{s}\}_n | \mathbf{J}, \mathbf{h}_n) P(\mathbf{J} | \bigcup_{i=1}^{n-1} \{\mathbf{s}_i, \mathbf{h}_i\})}{\sum_{\mathbf{J}} P(\{\mathbf{s}\}_n | \mathbf{J}, \mathbf{h}_n) P(\mathbf{J} | \bigcup_{i=1}^{n-1} \{\mathbf{s}_i, \mathbf{h}_i\})} \quad [12]$$

$$\log P_n = \log \mathcal{L}_n + \log P_{n-1} - \log Z_n \quad [13]$$

$$\frac{\partial \log P_n}{\partial J_{ij}} = \langle s_i s_j \rangle_n^o - \langle s_i s_j \rangle_n + \frac{\partial \log P_{n-1}}{\partial J_{ij}}. \quad [14]$$

average to replace the distribution average in Eq. 6. The procedure runs in an iterative way between computation and experiments, new perturbations are designed based on previous samples and our estimation of \mathbf{J} . Each time with new samples taken from the system, solving the optimization Eq. 16 gives the most informative perturbation to execute in the next experiment. This framework could also be expanded in the case of performing multiple new perturbations each time, with more terms of \mathbf{h}_n set as free decision variables. As the previous examples show, this optimization problem is highly complex and non-convex. In applications, we use a quasi-Newton method to find a reasonable choice of \mathbf{h} .

Results

Inference with oracle fields. First, we demonstrate that good perturbations can dramatically improve the precision of inference. Specifically, a medium-sized network can be deciphered with a few fields provided by an oracle that has a model of the underlying network. The oracle finds good perturbations by numerically optimizing Eq. 16 using the ground truth network, \mathbf{J} , and provides these perturbations to the inference procedure.

In many real systems, networks are composed of several communities or modules (18). One common form is a network that has activation inside each module and repression between different modules. For such systems, samples obtained from the natural condition are always inadequate to infer the exact position of these interactions. We performed our method on a 16-node network with three modules. The structure of the network is shown in Fig. 3 (a), and the weights are set as

random numbers to avoid special symmetry. As shown in Fig. 3 (b), some eigenvalues of FI of the original inference problem are as small as 10^{-10} . We take 5×10^6 samples from the distribution each time so there is no possibility to achieve accurate inference on the eigenvectors with 10^{-10} eigenvalues.

To demonstrate the existence of informative perturbations, \mathbf{h} , we perform numerical optimization of \mathbf{h} with the true \mathcal{I} and \mathbf{J} in Eq. 16, and use the resulting field as an oracle during the learning. The oracle fields are illustrated by a heatmap in Fig. 3 (c). After applying the field, the eigenvalues of FI are significantly increased by orders of magnitude. With only two perturbations, the smallest eigenvalue is around 10^{-4} , which is reasonable to infer with our sample size. We define two measures to quantify the improvement of inference after applying the perturbations. The mean estimation error is defined as $\sum_{i \neq j} |J_{ij} - \tilde{J}_{ij}| / (n(n-1))$, the training curve of which is showed in Fig. 3 (d). Denote the number of edges in the true network as K . We define the edge prediction precision to be the ratio of overlap between the most significant predicted K edges and the ground truth, as shown in Fig. 3 (e).

Without perturbation, the average prediction error of $\tilde{\mathbf{J}}$ does not decrease, as the improvement on correct edges is accompanied by false links in wrong edges. The edge prediction results can also be visualized by the heatmap of links shown in Fig. 3 (f). Prediction without perturbation is roughly all positive connections inside each module, and negative connections between modules. This phenomenon agrees with our intuition, that for strongly coupled networks we can only know the information of modules, but not the exact interactions inside and between modules. With two perturbations, the mean prediction error decreased to around 0.3, which is 10%

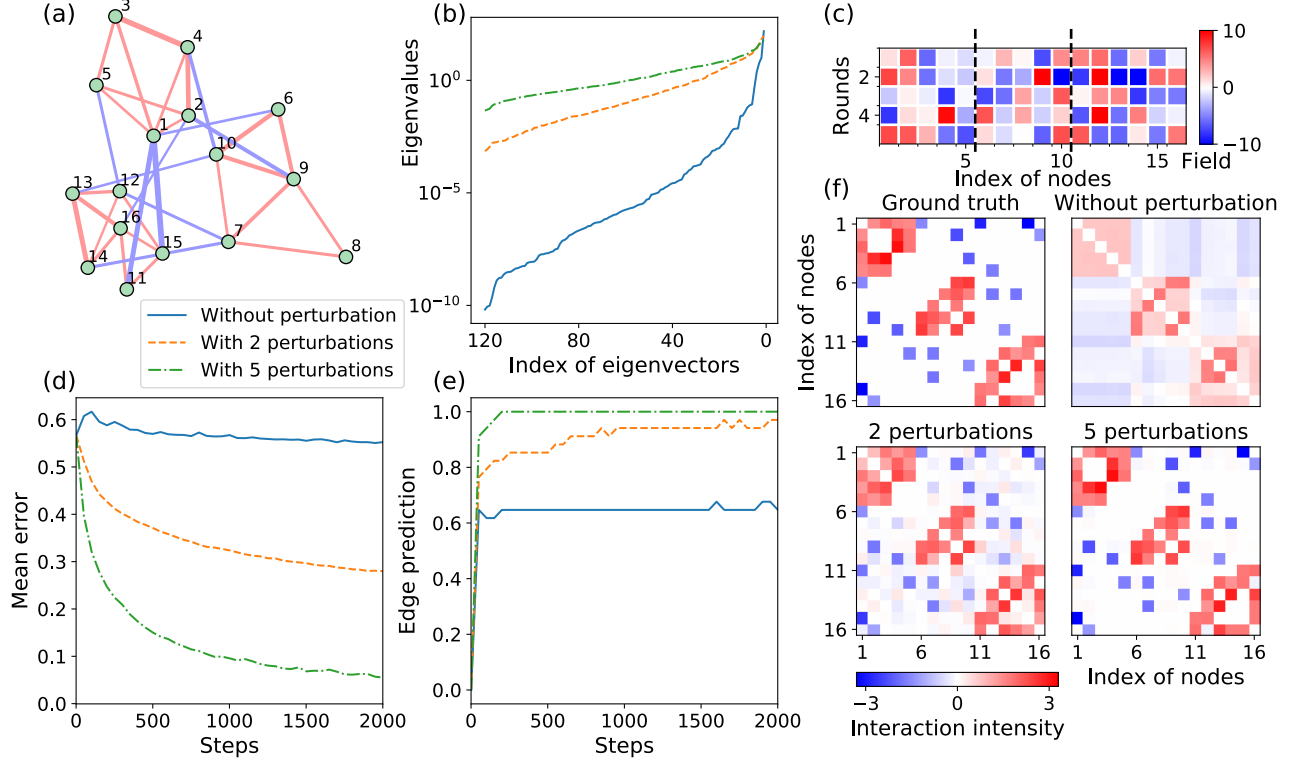


Fig. 3. Inference of a modular network with fields provided by an oracle. (a) Visualization of the structure of the network to be inferred. Red edges represent $J_{ij} > 0$ and blue edges represents $J_{ij} < 0$. The width of each edge is proportional to $|J_{ij}|$. (b) Eigenvalue spectrum of Fisher information matrix of the inference problem without perturbation and with a given number of perturbations. (b)(d)(e) share the same legend at the right side of (b). (c) Visualization of the applied perturbations. In the first round no perturbation is applied so there are 5 perturbations in total. The black dashed lines separate different modules in the network, and the modular structure can also be seen in (a). (d) Mean estimation error of J as a function of training steps. The total number of samples for each experiment is the same. (e) Edge prediction precision as a function of training steps. The strongest K edges in the prediction are compared with all the K edges of the real J to quantify the ratio of correct edges in the prediction. (f) Visualization of estimation of J . J and \tilde{J} are presented as heatmaps with $p \times p$ pixels.

of the mean interaction strength. Also, the prediction precision increases from 0.6 to around 1 compared with the case of no perturbation. So we could learn the structure of the network qualitatively with two perturbations. Moreover, with five perturbations, we can obtain quantitative knowledge of the network. The mean error of edge prediction goes down to 2% of the mean interaction strength, and prediction precision converges to 1 very quickly in the training, as shown in Fig. 3 (c)(e). The perturbations provided by the oracle procedure do not have an obvious pattern. In general, the perturbations try to break the strong coupling inside the module by forcing the nodes to have different values. Also, strong fields are applied to nodes that have more links in general.

Inference with inferred fields. The oracle method cannot be applied in real systems, as the structure of the network is unknown and an oracle that provides good perturbations will be unavailable in most cases. In real systems, to perform inference, we need to infer informative \mathbf{h} by using the empirical Fisher information and our estimation $\tilde{\mathbf{J}}$ in Eq. 4. To validate that our active learning method is still effective to find good perturbations, we perform the procedure in 49 randomly generated networks. Some examples of network structure are shown in Fig. 4 (a). The smallest eigenvalues of the original inference problem are around $10^{-7} \sim 10^{-10}$, therefore the inference is almost impossible with only 5×10^6 samples each

time.

The results show that the perturbations discovered using estimation from data can still reveal network structure. After each round of sampling, the training results of original problem and the perturbed problem are shown in Fig. 4 (b)(c). The mean training curves are shown in the opaque lines with standard deviation as error bar, and individual training curves are shown as transparent lines in the background. Without perturbation, after each round of sampling, the mean estimation error does not have observable change, and the prediction precision only improves slightly. In contrast, the training curves with our designed perturbations improve significantly as more samples are taken with different perturbations. For most networks, the edge prediction precision converges to 1 but with a different number of perturbations.

Even though inference in all networks is improved, the effect of 9 rounds of perturbation has some variation across networks. The final mean estimation error varies between 1% \sim 10% of the mean interaction strength. This is because our design of perturbation relies on the quality of estimation of \mathcal{I}, \mathbf{J} . For harder problems, our inference is more inaccurate, so the designed field is not as effective. The relation between the mean estimation error after 9 rounds of perturbation and the smallest eigenvalue of the inference problem without perturbation is shown in Fig. 4 (d). For inference without perturbation, the mean estimation error is insensitive to the

smallest eigenvalues, as information of these directions is never captured under the given sample size. In comparison, the final error with perturbations decreases significantly with larger smallest eigenvalues. For smallest eigenvalues around 10^{-9} , even though the number of samples is not sufficient to find the network structure, certain directions are pinned down where the inference is hard, so that we can use additional perturbations to improve accuracy. Previously, we showed that our knowledge of the system only increases with more perturbations, so we would expect convergence after enough rounds of perturbation.

In the process of finding a good \mathbf{h} , several approximations are made with some implicit assumptions. We argue that these approximations are valid in the sense of finding good perturbations. First, empirical FI is used instead of the true, accurate FI. By the theory of random matrices, the empirical FI converges to FI with increasing number of samples, and the convergence rate for different eigenvectors is proportional to the exponential of the eigenvalues (19). So we will have accurate FI estimation along those "easy" directions. Also, the estimation $\tilde{\mathbf{J}}$ is used in place of \mathbf{J} in computing \mathcal{I}_n . As FI is the expected Hessian of the log-likelihood function, by the theory of optimization, the convergence rates of the estimation is proportional to eigenvalues along different eigenvectors (20). In both cases, we will have good estimations along the eigenvectors whose eigenvalues are large. These are components of the interactions that our inference is accurate based on current samples, such as the positive interaction inside the module and negative interaction between modules. When designing new perturbations, we would like the new perturbation to reveal the information we have not obtained yet. Even though we do not have accurate knowledge for certain parts of a network, the discovered perturbations provide information about the directions along which our estimation is inadequate.

Discussion

In this paper, we developed a framework to rationally design and analyze perturbation experiments in networks. Our results show that perturbations designed to minimize the trace of inverse of FI (Fisher information) of the inference problem can provide significant improvements in both qualitative structure prediction and quantitative interaction strength estimation. Our framework combines statistical inference with active exploration, and thus mimics the scientific discovery process. Our method differs from traditional active learning methods. Traditional methods typically select new samples based upon uncertainty. Instead, we select perturbations that manipulate a given network to reveal information about the most uncertain properties. Many interesting statistical questions arise in this framework and need further exploration.

In practical situations where information about optimal perturbations is not available (Fig. 4), we use approximation on Eq. 16 to find a good choice of \mathbf{h} . Even though there are arguments that the discovered perturbation will still be informative under these approximations, strict analyses are still lacking. FI is widely recognized as a measure of the uncertainty in parametric inference, but the uncertainty in FI estimation is not as well-studied, which is essential in our case to know how good our proposed \mathbf{h} would be. Moreover, the sampling complexity of such a learning scheme has not been established. Results on specific examples studied here

show exponential improvement, but generalization to random networks needs more sophisticated analyses of underlying statistical questions.

We demonstrate that good choice of \mathbf{h} (using an oracle) yields dramatic improvements in inference in Fig. 3. In real situations, as we only have the samples taken from the system itself, the best possible perturbation should be defined in the sense of posterior distribution on all possible \mathbf{J} . Even these oracle \mathbf{h} enable more efficient inference depending on \mathbf{J} , trying to find such \mathbf{h} is in some sense impossible as we do not have the required information in \mathbf{J} . We could use the expected decrease of $\text{Tr } \mathcal{I}^{-1}$ on the posterior, or maximize the minimum improvements for a subset of the most possible \mathbf{J} .

Except for a few special cases, we find optimal fields numerically by finding fields that optimize the trace of the inverse of FI given the current estimate of network parameters. When applied to large networks, the optimization might be computationally intractable, and it would be more efficient if we could design \mathbf{h} directly from \mathbf{J} and \mathcal{I} without estimating the FI after hypothetical perturbation. Intuitively we would like the applied field to improve the probability of states that have not appeared before. Preliminary results on finding \mathbf{h} based on principal components analysis of the correlation matrix showed some utility, but further investigation is required to make this approach practical.

All the above analyses are based on the framework we proposed where we have full control of the field term, and can construct any possible field and then apply this field to the studied network. To apply our framework to real systems, our ability to perturb the system might be more constrained. For example, perturbations might be constrained in magnitude or in their ℓ_0 norm, which brings more challenges to theoretical analysis and optimization. Additionally, some central nodes could be essential to the proper function of the system and cannot be perturbed. Another possibility is that our control of \mathbf{h} is imprecise, that is we could set \mathbf{h} taken from a distribution. Moreover, the Ising model may not fully characterize the studied systems, as the symmetric interaction and equilibrium assumptions may not hold. Extending the understandings of the procedure to other models of complex networks would make the framework more powerful, such as Bayesian networks, dynamical systems, etc. We believe that our framework provides an interesting approach to design and analyze perturbations in order to improve our inference. The theoretical questions that arise in the process might provide new insights into statistical learning theory.

Materials and Methods

Numerical experiments were performed in MATLAB (21).

Learning of network parameters. For each round of learning, 5×10^6 examples are taken from the network by MCMC sampling. The optimization is performed by gradient ascent, and 5×10^3 samples are used in each step to estimate the gradient. The step size is chosen as $\eta = \lambda t^{-\alpha}$, where $\lambda = 0.1$, $\alpha \in [0.2, 0.5]$ depending on learning stages. To avoid over-fitting, ℓ_2 regularization is used during the training.

Generation of random networks. The random networks are generated by cutting off Gaussian random variables. Each edge is assigned a weight from the standard normal distribution, and we only keep the weights larger than 1.4 in magnitude. Then all remaining weights are rescaled to make their mean absolute value equal to 2.5.

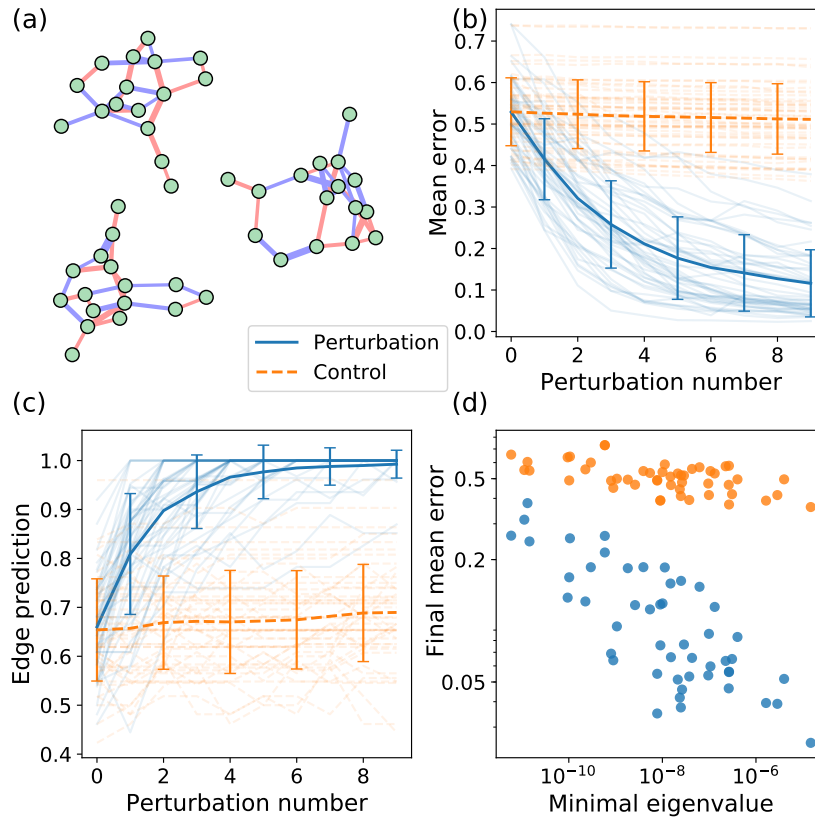


Fig. 4. Inference of random networks with inferred fields. (a) Examples of some random networks used in numerical experiments. (b) Mean estimation error after training is shown as a function of the number of applied perturbations for 16-node random networks. The opaque line and error bar represents the mean and standard deviation over all 49 tested random networks. The control group is set as taking the same extra number of samples but under the no perturbation condition. The transparent lines in the background show all trajectories for these networks. (c) Edge prediction precision is shown as a function of the number of applied perturbations. The definition is the same as in Fig 3 (e). Definition of opaque and transparent lines is the same as (b). (d) Log-log plot between the final mean estimation error and the smallest eigenvalue of FI of the system without perturbation.

Optimization of applied fields. For 16-node network, accurate Fisher information was used in the computation. When computing the trace of inverse, an identity matrix with 10^{-6} weight was added to avoid numerical instability. The optimization was performed by the optimization toolbox in MATLAB (21).

ACKNOWLEDGMENTS. The authors would like to thank Venkat Chandrasekaran and Andrew Stuart for influential discussions, and Yifan Chen for helpful suggestions. The authors would like to acknowledge support from the the Heritage Medical Research Institute (MT), the NIH (DP5 OD012194) (MT), and the Natural Sciences and Engineering Research Council (NSERC) Discovery Grant (DAS), and a Tier-II Canada Research Chair (DAS).

1. Le Novère N (2015) Quantitative and logic modelling of molecular and gene networks. *Nature Reviews Genetics* 16(3):146.
2. Nguyen HC, Zecchina R, Berg J (2017) Inverse statistical problems: from the inverse ising problem to data science. *Advances in Physics* 66(3):197–261.
3. Marks DS, et al. (2011) Protein 3d structure computed from evolutionary sequence variation. *PLoS one* 6(12):e28766.
4. Lezon TR, Banavar JR, Cieplak M, Maritan A, Fedoroff NV (2006) Using the principle of entropy maximization to infer genetic interaction networks from gene expression patterns. *Proceedings of the National Academy of Sciences* 103(50):19033–19038.
5. Cocco S, Leibler S, Monasson R (2009) Neuronal couplings between retinal ganglion cells inferred by efficient inverse statistical physics methods. *Proceedings of the National Academy of Sciences* 106(33):14058–14062.
6. Hinton GE, Osindero S, Teh YW (2006) A fast learning algorithm for deep belief nets. *Neural computation* 18(7):1527–1554.
7. Aurell E, Ekeberg M (2012) Inverse ising inference using all the data. *Physical review letters* 108(9):090201.
8. Vuffray M, Misra S, Lokhov A, Chertkov M (2016) Interaction screening: Efficient and sample-optimal learning of ising models in *Advances in Neural Information Processing Systems*. pp. 2595–2603.
9. Santhanam NP, Wainwright MJ (2012) Information-theoretic limits of selecting binary graphical models in high dimensions. *IEEE Trans. Information Theory* 58(7):4117–4134.
10. Montanari A, Pereira JA (2009) Which graphical models are difficult to learn? in *Advances in Neural Information Processing Systems*. pp. 1303–1311.
11. Watanabe S (2009) *Algebraic geometry and statistical learning theory*. (Cambridge University Press) Vol. 25.

12. Hsu PD, Lander ES, Zhang F (2014) Development and applications of crispr-cas9 for genome engineering. *Cell* 157(6):1262–1278.
13. Dixit A, et al. (2016) Perturb-seq: dissecting molecular circuits with scalable single-cell rna profiling of pooled genetic screens. *Cell* 167(7):1853–1866.
14. Deisseroth K (2011) Optogenetics. *Nature methods* 8(1):26.
15. Ideker TE, THORSSON V, Karp RM (1999) Discovery of regulatory interactions through perturbation: inference and experimental design in *Biocomputing 2000*. (World Scientific), pp. 305–316.
16. Hyttinen A, Eberhardt F, Hoyer PO (2013) Experiment selection for causal discovery. *The Journal of Machine Learning Research* 14(1):3041–3071.
17. Molinelli EJ, et al. (2013) Perturbation biology: inferring signaling networks in cellular systems. *PLoS computational biology* 9(12):e1003290.
18. Newman ME (2006) Modularity and community structure in networks. *Proceedings of the national academy of sciences* 103(23):8577–8582.
19. Tropp JA, et al. (2015) An introduction to matrix concentration inequalities. *Foundations and Trends® in Machine Learning* 8(1-2):1–230.
20. Boyd S, Vandenberghe L (2004) *Convex optimization*. (Cambridge university press).
21. (R2018b) MATLAB, version 9.5.0.942161. The MathWorks Inc., Natick, MA, USA.